Adam MUC[1], Jan IWASZKIEWICZ[2]

Uniwersytet Morski w Gdyni, Katedra Automatyki Okrętowej (1,2)
ORCID: 1. 0000-0002-9495-087X; 2. 0000-0002-9827-715X

doi:10.15199/48.2024.05.15

Three-phase Cascade Inverter Controlled by Signals Calculated based on the Haar Wavelet

Streszczenie. *W artykule opisano syntezę wartości chwilowej napięcia wyjściowego wielopoziomowego trójfazowego falownika kaskadowego. Opisano analityczną metodę wyznaczania zbioru falek ortogonalnych Haara oraz propozycję syntezy przebiegów wyjściowych falownika w oparciu o transformatę falkową. Na podstawie falki Haara obliczono sygnały sterujące kluczami połączonych kaskadowo dwupoziomowych falowników tworzących wielopoziomowy trójfazowy falownik napięcia. Przeprowadzono symulację współpracy takiego falownika z obciążeniem rezystancyjno-indukcyjnym. (**Trójfazowy falownik kaskadowy sterowany wektorami obliczonymi na podstawie falki Haara**).*

Abstract*. The article describes the synthesis of the instantaneous value of the output voltage of a multi-level three-phase cascade inverter. An analytical method for determining the set of Haar orthogonal wavelets and a proposal for synthesizing the inverter's output waveforms based on the wavelet transform are described. Based on the Haar wavelet, the control signals of the keys of the cascaded two-level inverters forming a multi-level three-level voltage inverter were calculated. The cooperation of such an inverter with a resistive-inductive load was simulated.*

Słowa kluczowe: falka Haara, transformata falkowa, falownik wielopoziomowy, falownik trójfazowy, synteza przebiegów falkowych.
Keywords: Haar wavelet, wavelet transform, multilevel converter, three-phase inverter, wavelet waveforms synthesis.

Introduction

Over the past few decades, inverters have become a popular technology. The great interest in optimizing and improving the efficiency of inverters is justified by the continuous demand for their use in various industry sectors, such as electric drives, power systems, and renewable energy systems. One of the goals of this research effort is to develop and experimentally test electronic key-switching techniques that allow the control of inverters to produce input signals with reduced harmonic content, regardless of their ratings, configurations, types, and load conditions. Several inverter-switching techniques have been described in the literature and have been developed and tested to support both single-phase and three-phase inverters [1,2].

Devices such as voltage and current converters are now able to control and power a variety of devices operating in the power range of hundreds of kW and more. These devices have to fulfil definite and diversified requirements which implies diversified purposes and methods of electric energy conversion. There are many industrial applications e.g. uninterruptible power supplies (UPS) or distributed power generation systems, where the essential demand is to generate 50 or 60 Hz sinusoidal voltage waveforms. The quality of generated waveforms, especially the Total Harmonic Distortion factor (THD), should comply with appropriate standards. In many devices like UPSs, active filters, or voltage regulators in electric energy grids, the most important features are high-quality output waveforms, output stability, and efficiency of the device [3, 4]. Similar requirements are to be fulfilled in converters applied in renewable energy systems.

Pulse width modulation (PWM) is a key technique used with inverters. PWM is used to switch and operate inverters and controlled converters to produce higher-quality output voltages and currents for various loads. Using modulation techniques, we can control the electronic keys to get the desired amplitude and frequency. To date, several modifications to the typical PWM technique have been proposed. The most popular PWM modifications are sinusoidal pulse width modulation (SPWM), random pulse width modulation (RPWM) and space vector modulation (SVM). The main problem resulting from the use of PWM is the problem of higher harmonics, which can lead to damage to the inverter, noise, motor failure, increase in torque pulsation or increase in motor temperature and shorten its life [2].

The features, performance, drawbacks, and limitations of the VSI inverter have been largely recognized and verified in practice. Latest achievements in power semi-conductor technology permit it to work with higher frequency but fast switching accompanying the PWM control causes power losses in switching elements thus cutting inverter efficiency down [5].

Recently, multilevel inverters have emerged as a new and very important class of converters. Thanks to their promising performance, multilevel inverters are becoming more and more an alternative to conventional two-level inverters. They permit us to overcome the problem of limited power and shape output waveforms. As a result, many multilevel converters have been applied in the industry.

The development of multilevel converters comprises a novel area of research for new topologies, control strategies, and theory. Producing the required voltage or current waveforms is possible in many ways: e.g. sinusoidal PWM, selective harmonic elimination, space-vector modulation (SVM), or shaping the stepped voltage or current [6, 7]. Important works and studies concern the subject of frequency adjustment. Diverse methods of converters' control such as computing the adequate switching angles of stepped waveforms or cutting specified harmonics have been developed [7]. Using PWM methods provokes decreasing converter efficiency, which is a serious disadvantage, particularly in higher-power applications.

The aforementioned disadvantages can be slightly reduced by the use of novel converters topologies as well as mathematical tools-aided control strategies. The paper deals with the technique of shaping the stepped output waveforms in multilevel converters. A mathematical approach to the control strategy based on wavelet transforms is presented. The output waveform synthesis is accomplished using a set of orthogonal wavelets. The discussion includes such mathematical tools as the Haar wavelet transform [7,8,9]. In particular, in [9] the approximation of the sin(x) function was considered using various methods, for example, the approximation of the sin(x) function using Haar wavelets was compared with functions using the Fourier series. The article presents the initial simulation studies of the developed single-phase

inverter model controlled by wavelet signals. This is the first model that enables the implementation of the wavelet theory presented in [8,9]. The next step will be an attempt to implement the presented inverter and experimental research.

Wavelet waveforms synthesis

Wavelets is a term for mathematical functions, that allow the analysis of signals in different time scales and resolutions. The wavelet applications are in many not directly related areas like seismology, video analysis, quantum mechanics, or electronics. The wavelets have been used mainly for analysing processes or signals based on the decomposition of the elements of the processes. The following considerations will prove that wavelets can also be useful in the composition of power electronics signals and structures. The main application of the wavelet theory is used in control algorithms [10,11,12,13] or diagnostics [14,15] and the detection [16] of various types of faults in converters, networks, or drives [2]. The Haar wavelet, on the other hand, is not so widely used.

The Haar wavelets have been adapted [6,7] for cascade inverter control. The Haar wavelet form is similar to the form of the voltage or current pulse that can be obtained using a simple one-phase inverter i.e. H-bridge cell. The displacement and width of the wavelet can be freely created and controlled. Thanks to these properties it is possible to apply wavelets in power electronics e.g. to form the output stepped waveforms of multilevel converters [16].

Let us define the scaling function $\varphi(x)$ in an interval $x\in<0,2\pi)$:

$$\varphi(x)=\left\{\begin{array}{llll} 1 & \text{for} & 0\le x<2\pi, \\ 0 & \text{for} & \text{other} \quad x \end{array}\right\} \tag{1}$$

The fundamental proposed wavelet is defined:

$$\psi(x)=\left\{\begin{array}{llll} 1 & \text{for} & 0\le x<\pi, \\ -1 & \text{for} & \pi\le x<2\pi, \\ 0 & \text{for} & \text{other} \quad x \end{array}\right\} \tag{2}$$

The wavelet determines one period of the rectangular wave and is the mother function introducing a family of wavelets:

$$\psi_{mn}(x)=\psi\left(2^{-m}x-2\pi n\right) \quad \text{for} \quad m,n=\ldots,-2,-1,0,1,2,\ldots \tag{3}$$

The wavelet scale is done as $2^m 2\pi$ and its displacement on the x-axis is determined as n-times $2^{m+1}\pi$. The m factor scales not only the wavelet but the amplitude too.

The scaling function and a few wavelets have been presented in Figure 1.

All wavelets $\psi_{mn}(x)$ are orthogonal in the interval $x\in<0,2\pi)$. The defined statement (7) creates a family of orthogonal functions and can determine the basis of the wavelet transform. A continuous wavelet transform is defined as:

$$Wf(m,n)=\int_{-\infty}^{\infty} f(x)\psi_{mn}(x)\,\mathrm{d}x \tag{4}$$

and presents itself as a scalar product of functions $f(x)$ and function $\psi_{mn}(x)$. The function f(x) reconstruction occurs when the inverse wavelet transform is applied (5).

In applications more comfortable is using a discrete inverse wavelet transform which is defined according to (6) by the equation:

$$f(x)=C\sum_{m=-\infty}^{\infty}\sum_{n=-\infty}^{\infty} Wf(m,n)\psi_{mn}(x) \tag{5}$$

The symbol C denotes a constant that can be calculated from the Fourier transform of the function $\psi_{mn}(x)$. It could be written as a sum of wavelets $\psi_{mn}(x)$ multiplied by coefficients a_{mn}

$$f(x)=\sum_{m=-\infty}^{\infty}\sum_{n=-\infty}^{\infty} a_{mn}\,\psi_{mn}(x) \tag{6}$$

The coefficients a_{mn}, called wavelet coefficients, are scalar products of the function $f(x)$ and wavelets $\psi_{mn}(x)$. In the interval $x\in<0,2\pi)$ they are given as

$$a_{mn}=C_m\int_0^{2\pi} f(x)\psi_{mn}(x)\,\mathrm{d}x \tag{7}$$

The constant C_m is only dependent on coefficient m and has the same value for different n. Denoting

$$f_{mn}(x)=a_{mn}\,\psi_{mn}(x) \tag{8}$$

it is possible to write $f_\psi(x)$ as a sum of components $f_{mn}(x)$:

$$f_\psi(x)=\sum_{m=-3}^{m=0}\sum_{n=0}^{2^{-m}-1} f_{mn}(x) \tag{9}$$

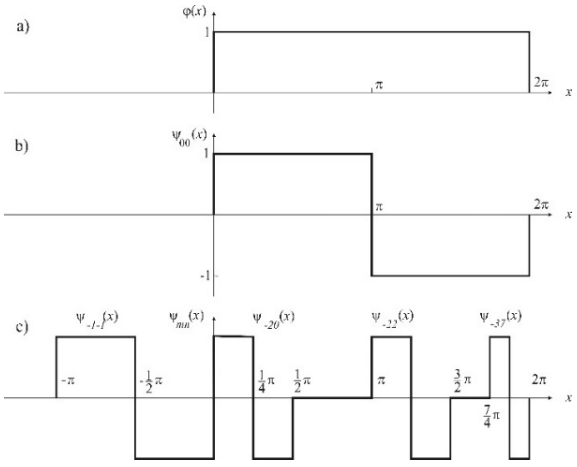

Fig.1. The scaling function $\varphi(x)$ and wavelets $\psi_{mn}(x)$: a) scaling function $\varphi(x)$, b) fundamental wavelet $\psi_{00}(x)$, c) wavelets $\psi_{-1\text{-}1}(x)$, $\psi_{-20}(x), \psi_{-22}(x), \psi_{-37}(x)$

The components are $f_{mn}(x)$ present component wavelets, amplitude, and phase which are determined by coefficients a_{mn}, calculated according to (7).

In power electronics, the most important criterion of the approximated waveforms is the THD factor. Practically in power electronics applications, the approximation of a sine wave should be realized using a finite number of wavelets. The natural aspiration of designers is to utilize the possibly lowest number of components. The accuracy of approximation depends on it. In mathematics, the accuracy is determined as an average square error δ, a very useful criterion destined for that purpose.

Let us denote by $f_\psi(x)$ a waveform approximating the function $f(x)=\sin(x)$ in the interval $x\in<0,2\pi)$. Assuming that $f_\psi(x)$ forms a combination of wavelets determined by index m = -3, -2, -1, 0 it can be written as a sum:

(10) $$f_{\psi}(x)=\sum_{m=-3}^{m=0}\sum_{n=0}^{2^{-m}-1}a_{mn}\,\psi_{mn}(x)=\sum_{m=-3}^{m=0}\sum_{n=0}^{2^{-m}-1}f_{mn}(x)$$

All coefficients a_{mn}, calculated according to (7), have been collected in Table 1.

a)

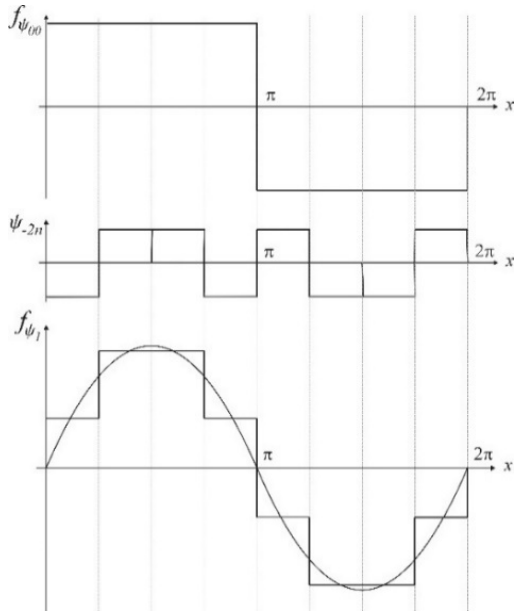

b)

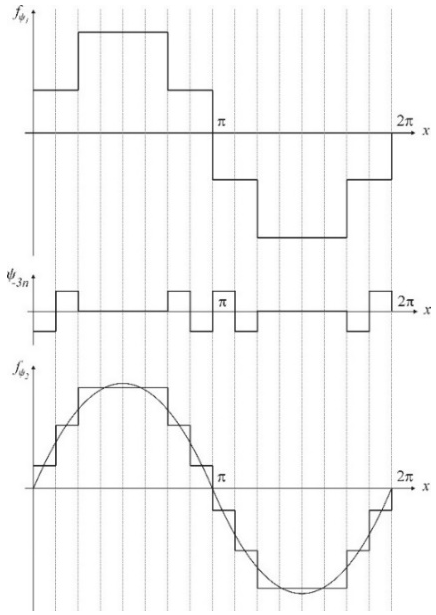

Fig. 2. The first step of wavelet approximation (a): $f_{\psi_1}(x)=f_{-20}+f_{-21}+f_{-22}+f_{-23}+f_{00}$, and the second step of wavelet approximation (b): $f_{\psi_2}(x)=f_{-30}+f_{-33}+f_{-34}+f_{-37}+f_{\psi 1}$

Table 1. The wavelet coefficients a_{mn}.

a_{mn}	n					
	0	1	2	3	4	5
a_{0n}	0.636	–	–	–	–	–
a_{-1n}	0	0	–	–	–	–
a_{-2n}	- 0.264	0.264	0.264	- 0.264	–	–
a_{-3n}	- 0.179	- 0.074	0.074	0.179	0.179	0.074

Successive steps of wavelet approximation $f_{\psi k}(x)$ for $k = 1, 2, 3$ have been presented in Figures 2, 3, and 4. The first step of reconstruction creates function $f_{\psi 1}(x)$ as a set of wavelets:

(11) $$f_{\psi_1}(x)=\sum_{m=-2}^{m=0}\sum_{n=0}^{2^{-m}-1}f_{mn}(x)$$

and

(12) $$f_{\psi_1}(x)=f_{-20}+f_{-21}+f_{-22}+f_{-23}+f_{-10}+f_{-11}+f_{\psi_0}(x)$$

in which two component wavelets are equal to zero according to Table 1. The waveforms are presented in Figure 2 (a). Figure 2 (b) presents the result of the second step of approximation in which a few (but not all) wavelets f_{-3n} have been added to the function $f_{\psi 1}(x)$. Function $f_{\psi 2}(x)$ creates a composition of the following wavelets:

(13) $$f_{\psi_2}(x)=f_{-30}+f_{-33}+f_{-34}+f_{-37}+f_{\psi_1}(x)$$

Wavelet converter

The topology of the cascade inverter was used to build a three-phase voltage inverter controlled by wavelet signals. For the first wavelet form, a three-phase voltage inverter consists of three two-level and single-phase voltage inverters (Fig. 3). There must be six inverters for two wavelet forms, and for three wavelet forms, there must be nine. In Figure 3, capital letters "A", "B" and "C" are assumed to denote components of the system, e.g. control blocks, load, etc. for a specific phase. The lowercase letters "a", "b" and "c" were used to describe the signals. In the further part of the study, examples of voltage and current waveforms mainly concern phase A.

In Figure 3, the blocks marked "inverter control" mean systems that form control signals for a given level of single-phase inverters. These blocks between the phases are the same - which makes the control system simple. The numbers entered next to the designation of system elements (e.g. the first number for transformers, the number in the "inverter control" block) means the next level of inverters in the created cascade. The block labeled "frequency" is the source of the triangular carrier signal. For each phase, these signals differ only in phase shift. The block marked "segments" is used by the logic of the "inverter control" block to determine the number of rectangular components forming a given wavelet signal. For the considered range of wavelets, only 16 segments are enough to reconstruct the shape of the function from Figures 1 and 2.

The article shows the shape of the output voltage using three wavelet forms that create the output voltage in each of the three phases. According to the authors, the output voltage reproduces the shape of the sinusoidal function with high accuracy. As part of the simulation tests, three-phase voltage and current waveforms for three variants were shown. In the first variant, only the first wavelet form was used. In the second variant, the first and second wavelet forms were used, and in the third variant, three wavelet forms were used, which were mathematically described in the theoretical part of the article.

The proposed method based on wavelet transform is very suitable for cascade converters even though it demands independent voltage sources. In each phase of the complex converter, the component inverters are supplied from three independent voltage sources: U_{D1}, U_{D2}, and U_{D3}. The supply voltages are proportional to the relevant amplitudes of component wavelets. If the proportional factor is set to 500 the voltage U_{D1} = 318 V, U_{D2} = 132 V, and U_{D3} = 84 V.

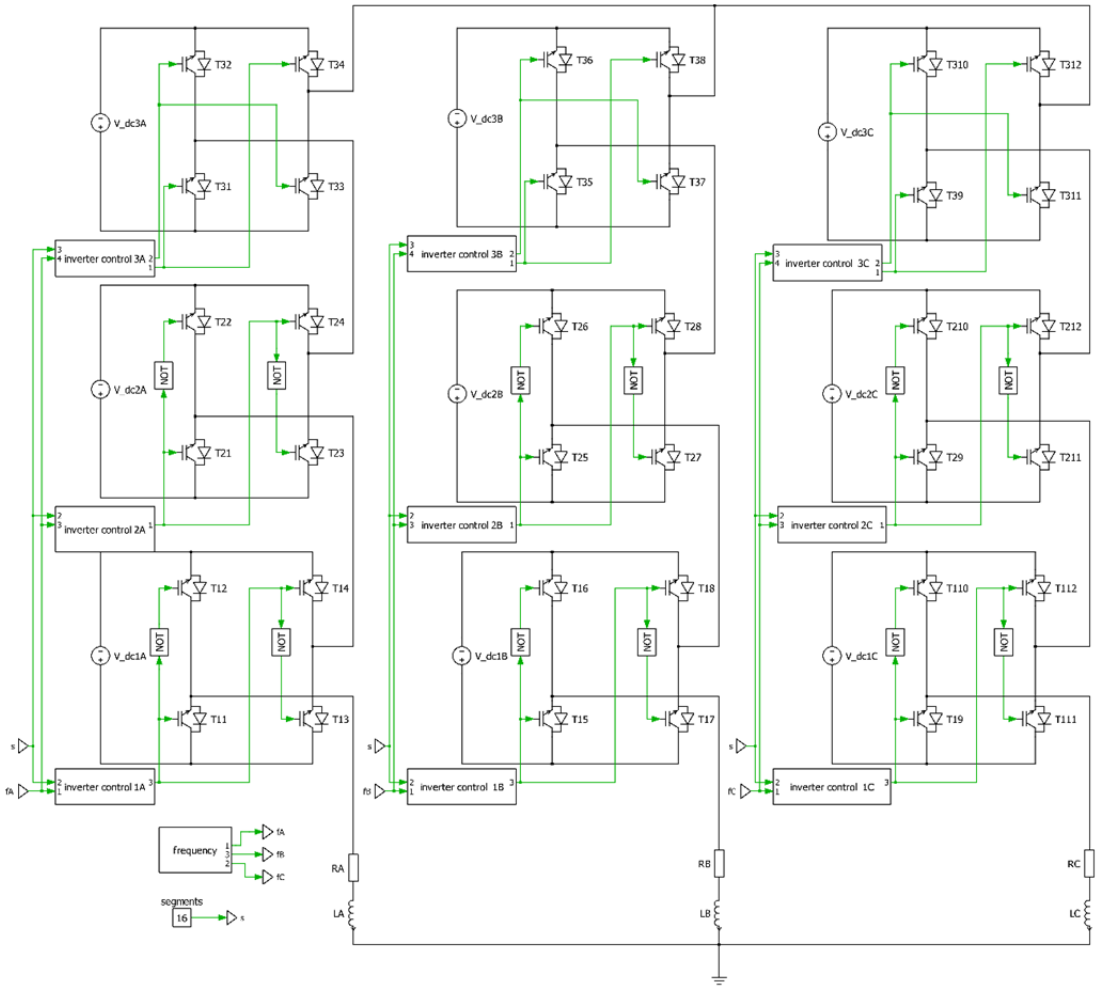

Fig.3. Three-phase cascade inverter controlled by wavelet signals

The control of such a converter is derived from the described wavelets model. The inverter control signals, which were calculated from the Haar wavelet, are shown in Figure 4. The designation of the control signals in Figure 4 is consistent with the designation of the transistors in Figure 3. Figure 4 shows only those signals that differ, the other control signals for a given inverter are created by negation. For the remaining phases, i.e. phases B and C, the signals are similar except for the phase shift of 120˚ and 240˚ degrees. These are control signals derived for the A phase and for three wavelet levels. The first inverter, counting from the top, generates the output voltage with the waveform $f_{\psi 00}$, the second with the waveform ψ_{-2n}, and the third with the waveform ψ_{-3n}.

The summing process of the wavelets in the cascade is accomplished by serially connecting the outputs of the component inverters whose switching frequencies differ. The fundamental frequency is 50 Hz, the frequencies of individual wavelets are different and take the following values: for $f_{\psi 00}$ is f = 50 Hz, for ψ_{-2n} is f = 200 Hz, for ψ_{-3n} is f = 400 Hz. For example, for wavelet ψ_{-2n} due to the phase change, there will appear pulses of 5 ms duration two times in each output voltage period, and for wavelet ψ_{-3n} appear pulses of 2.5 ms duration.

Simulation tests were carried out in the PLECS program and the RT Box device, which enables HIL (hardware in the loop) simulations. In simulation tests, the cooperation of the proposed inverter with resistive-inductive load was checked. An interesting situation occurs with resistive-inductive loads.

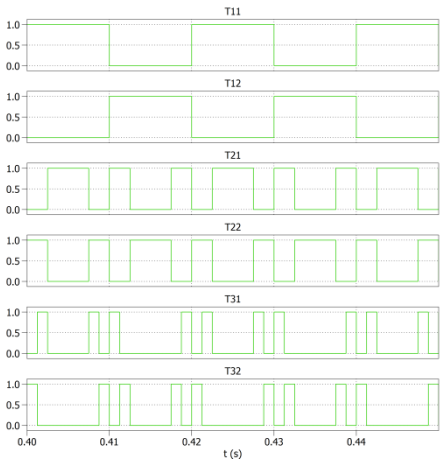

Fig. 4. Control ranges of individual transistors in a single-phase six-level voltage inverter system realizing the wavelet model of the converter

Figures 5, 6 and 7 show examples of voltages and current waveforms at the same load R_0 = 15 Ω and L_0 = 30 mH and for the fundamental frequency f = 50 Hz.
The waveforms obtained in Figure 5 are typical for the case of simple control for a three-phase two-level inverter. The same remark applies to spectra. In addition, the figure with the spectra (Fig. 5b) shows the DC component of the current, which is not a desirable effect of the waveguide operation.

By introducing successive levels in the cascade inverter together with successive shapes of wavelets, the shape of the voltage and current is closer to the sine function.

In the research on the single-phase inverter described in [17], the shape of the output voltages was closer to the function calculated in Figures 1 and 2.

The spectral characteristics shown in Figure 6 (b) show the influence of the seventh harmonic at the level of about 2%, while for the case with three levels of inverters, the level of higher current harmonics is practically not recorded (Fig. 7 (b)).

a)

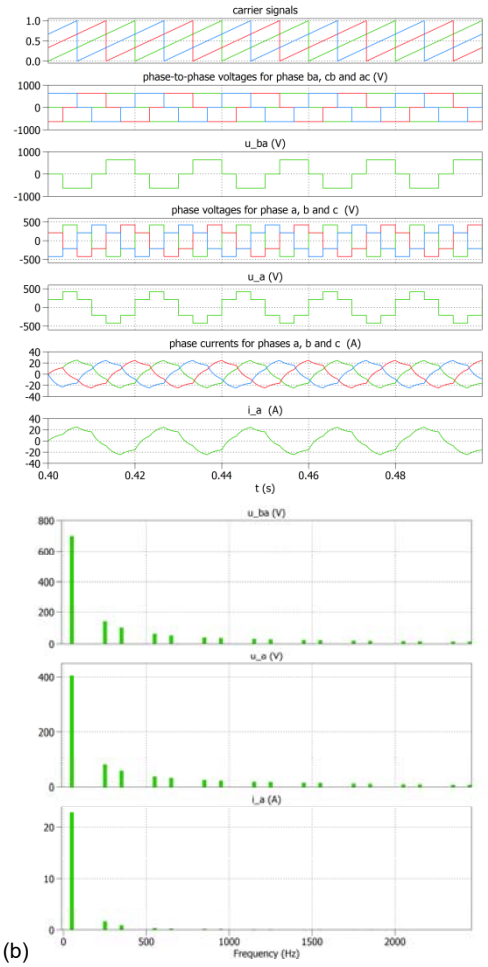

(b)

Fig. 5. Waveforms of voltages and currents for the first step of the wavelet approximation (a) and their spectrum (49 harmonics) (b)

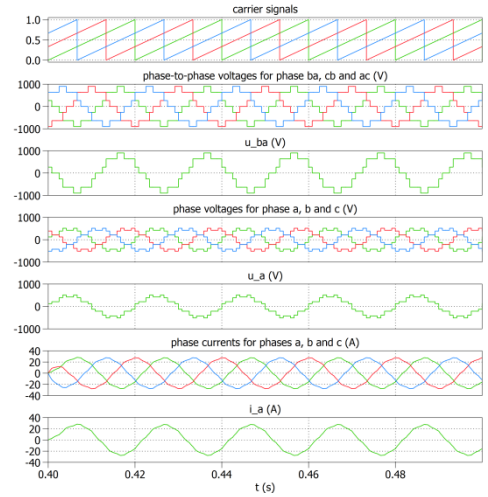

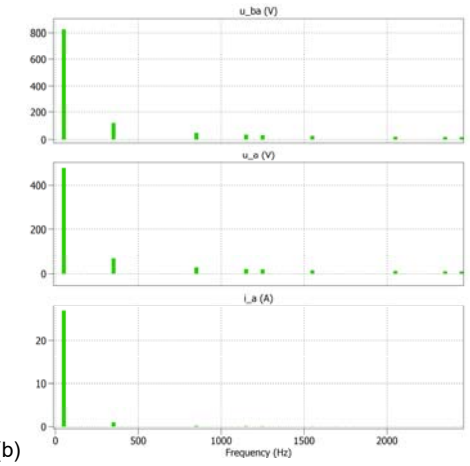

(b)

Fig. 6. Voltage and current waveforms for the second step of the wavelet approximation (a) and their spectrum (b).

a)

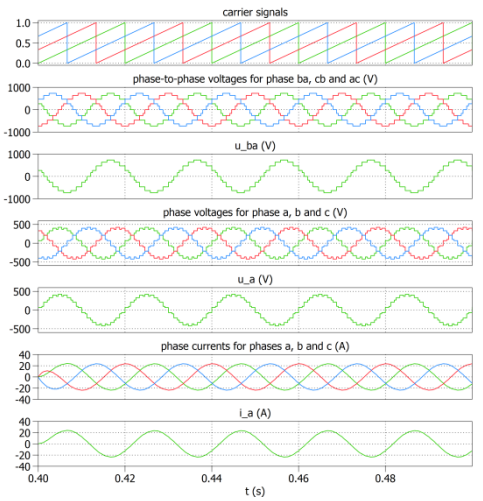

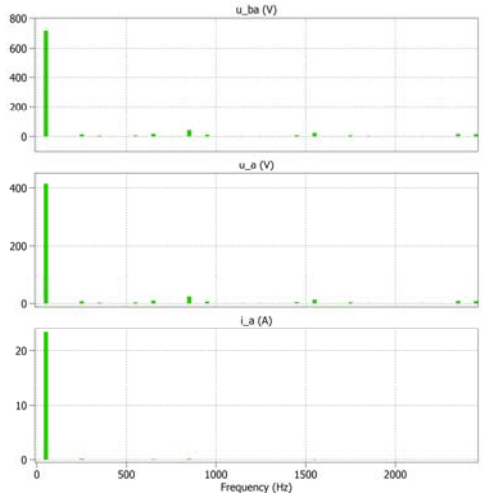

(b)

Fig. 7. Voltage and current waveforms for the third step of the wavelet approximation (a) and their spectrum (b).

Selected parameters of the output voltages and currents of the cascade inverter for the considered wavelet signals used in the control are listed in Table 2. In particular, the RMS and THD values were focused on. As can be seen from the presented results, along with the complication of the control with successive wavelet functions, the THD content in the case of voltages and currents is significantly reduced. However, an interesting situation occurs in the case of the RMS value, especially in the second case

(Figure 6), where we observe an increase in the RMS value. This is probably due to the summative nature of the second wavelet function.

Table 2. Selected parameters of voltages and currents for the considered wave functions

Case	RMS u_oa (V)	THD u_oa (%)	RMS i_oa (V)	THD i_oa (%)
Figure 5	299.81	31.10	16.20	8.3
Figure 6	341.01	18.15	18.95	3.8
Figure 7	293.91	9.15	16.52	1.0

Conclusion

The three-phase cascade inverter controlled by signals calculated based on the Haar wavelet allows obtaining a waveform of the output voltage with a very low content of THD without using PWM modulation and additional filters. On the other hand, an RL load with a low inductance value allows us to obtain a current waveform similar to a sine wave with a low THD = 4.4 %. As a result, the proposed system with wavelet control is an interesting proposition in the case of intensively developing systems with multi-level inverters in renewable energy sources.

The presented simulation studies encourage the implementation of this control strategy in a real system. Tests in the real system are very real because to build a cascade inverter with the topology shown in Figure 3, very popular single-phase H-bridge inverter systems are needed.

***Autors**: dr hab. inż. Jan Iwaszkiewicz, E-mail: j.iwaszkiewicz@we.umg.edu.pl; dr inż. Adam Muc, E-mail: a.muc@we.umg.edu.pl, Gdynia Maritime University, Department of Ship Automation, FACULTY OF ELECTRICAL ENGINEERING, 81-87 Morska St., 81-225 Gdynia.*

LITERATURE

[1] Chiasson J. N., Tolbert L. M., McKenzie K. J., Zhong Du.: Control of a Multilevel Using Resultant Theory. IEEE Transactions on Control Systems Technology, (2003), vol. 11, no. 3,

[2] Eswar K. N. D. V. S., Doss M. A. N., Vishnuram P., Selim A., Bajaj M., Kotb H., Kamel K., Comprehensive Study on Reduced DC Source Count: Multilevel Inverters and Its Design Topologies, Energies, (2023), 16, 18. https://doi.org/10.3390/en16010018

[3] Daubechies I.: The wavelet Transform, time-frequency localization and signal analysis. IEEE Transactions on Informatics Theory, (1990), vol. 36, pp. 961-1005

[4] Faranda R., Valade I.: UPQC Compensation Strategy and Design Aimed at Reducing Losses. IEEE International Symposium on Industrial Electronics ISIE (2002), vol. 4, pp. 1264-1270

[5] Graps A.: An Introduction to Wavelets, IEEE Computa-tional Science and Engineering, (1995), vol. 2, no. 2.

[6] Haar A.: Zur Theorie der orthogonalen Funktionensysteme, Mathematische Annalen, 1910, Vol. 69, pp. 331-371

[7] Muc A., Iwaszkiewicz J., Active Filtering of Inverter Output Waveforms Based on Orthogonal Space Vector Theory, Energies 2022, 15(21), 7861, https://doi.org/10.3390/en15217861

[8] Iwaszkiewicz J., Perz J. – „A Novel Approach to Control of Multilevel Converter Using Wavelets Transform", RE&PQJ, Vol. 1, No.5, March 2007, https://doi.org/10.24084/repqj05.371

[9] Iwaszkiewicz J., Modele matematyczne energoelektronicznych przekształtników wielopoziomowych. Analiza właściwości i zastosowanie, Wyd. Sieć Badawcza Łukasiewicz - Instytut Elektrotechniki, Z. 227, (2006), pp. 1-142

[10] Dwivedi U. D., Tiwari C., A generalised wavelet modulation scheme for single-phase inverters, 2015 International Conference on Energy, Power and Environment: Towards Sustainable Growth (ICEPE), Shillong, India, 2015, pp. 1-6, doi: 10.1109/EPETSG.2015.7510129

[11] Saleh S. A., Rahman M. A., Development and Testing of a New Controlled Wavelet-Modulated Inverter for IPM Motor Drives, in IEEE Transactions on Industry Applications, vol. 46, no. 4, pp. 1630-1643, July-Aug. 2010, doi: 10.1109/TIA.2010.2049814

[12] Saleh S. A., Balancing Capacitor Voltages in 7-Level Single Phase Flying-Capacitor Wavelet Modulated Inverters, 2022 IEEE Industry Applications Society Annual Meeting (IAS), (2022), 10.1109/IAS54023.2022.9939910

[13] George T., Jayaprakash P., Subramaniam U., Almakhles DJ, Frame-Angle Controlled Wavelet Modulated Inverter and Self-Recurrent Wavelet Neural Network-Based Maximum Power Point Tracking for Wind Energy Conversion System, w: IEEE Access, tom . 8, s. 171373-171386, 2020, doi: 10.1109/ACCESS.2020.3025309.

[14] Gong X., Wang N., Zhang Y., Yin S., Wang M., Wu G., Fault Diagnosis of Micro Grid Inverter Based on Wavelet Transform and Probabilistic Neural Network, 2020 39th Chinese Control Conference (CCC), Shenyang, China, 2020, pp. 4078-4082, doi: 10.23919/CCC50068.2020.9188646

[15] Chen D., Ye Y., Hua R., Fault diagnosis of three-level inverter based on wavelet analysis and Bayesian classifier, 2013 25th Chinese Control and Decision Conference (CCDC), Guiyang, China, 2013, pp. 4777-4780, doi: 10.1109/CCDC.2013.6561798.

[16] Eddine Ch. B. D., Azzeddine B., Mokhtar B., Detection of a two-level inverter open-circuit fault using the discrete wavelet transforms technique, 2018 IEEE International Conference on Industrial Technology (ICIT), (2018), 10.1109/ICIT.2018.8352206

[17] Muc A., Iwaszkiewicz J., Piechowski L., Single-phase Cascade Inverter Controlled By Vectors Calculated From The Haar Wavelet, Materiały konferencyjne w: XXII Krajowa Konferencja Elektroniki, Darłowo, 11-15.06.2023r.